

Exchange-dependent hybridization at the Pd-Fe interface

O. Rader,* C. Carbone, W. Clemens, E. Vescovo, S. Blügel, and W. Eberhardt

Institut für Festkörperforschung, Forschungszentrum Jülich GmbH, Postfach 1913, W-5170 Jülich, Germany

W. Gudat

Berliner Elektronenspeicherring-Gesellschaft für Synchrotronstrahlung mbH, Lentzeallee 100, W-1000 Berlin 33, Germany

(Received 18 February 1992)

We have studied the spin-polarized electronic structure of 1–4 monolayers (ML) of Pd on Fe(100). Pd grows epitaxially and without interdiffusion on top of Fe(100) up to 2 ML. Spin- and angle-resolved valence-band photoemission spectra show that 1-ML Pd is ferromagnetically ordered. An exchange splitting cannot directly be determined from the positions of the maxima in the spin-resolved spectra. The results are explained on the basis of our *ab initio* full-potential linear augmented-plane-wave calculation. The majority and minority spin electronic structures of the overlayer are found to be very differently affected by the Pd4*d*–Fe3*d* interface hybridization.

The electronic properties of palladium metal have often been identified as the reason for astonishing magnetic phenomena. While the electron configuration of the Pd *atom* is $4d^{10}5s^0$, in the *solid* the electrons rearrange to form $4d^{8.7}5s^{0.6}5p^{0.7}$ and to convert the diamagnetic atoms to a metal that exhibits an extraordinarily large experimental paramagnetic susceptibility.¹ The susceptibility of Pd is strongly enhanced by exchange interaction² with a Stoner enhancement factor of about 10, so that Pd can be considered almost ferromagnetic. Therefore, one expects that ferromagnetic 3*d* metals brought into contact with Pd induce large magnetic polarizations. Indeed, contact between Pd and Fe in dilute PdFe alloys is known to produce large magnetic polarization clouds generally referred to as “giant moments.”³ Similar polarization effects of Pd have been found for sputtered and epitaxial Fe-Pd multilayers.⁴

Recent nonrelativistic calculations⁵ predict that a lattice expansion by 5% to 6% will render Pd ferromagnetic because of the sensitive dependence of the *s*-*d* hybridization on the lattice constant. In Ref. 6 various attempts to verify this prediction experimentally have been reviewed. In view of their mostly negative results, Celinski *et al.*⁷ combined the effect of stretching Pd laterally by 5.1% with that of the Pd-Fe interface when growing Fe/Pd/Fe/Ag(100) sandwiches and obtained up to four ferromagnetically ordered Pd layers in this system.

Recently spin-resolved photoemission has been applied to study the electronic structure at the Pd(111)-Fe(110) interface by Weber *et al.*⁸ Surprisingly, they observed a spin splitting inverted with respect to that of Fe. Still, the question whether and how hybridization, as the authors suggested, can be identified as the origin of this structure could not be answered conclusively because the appropriate band-structure calculation is unavailable. A different interpretation, based on a totally different *magnetic* structure, i.e., antiferromagnetic coupling between overlayer and substrate, still appeared possible.

For our spin- and angle-resolved photoemission study we have chosen the system 1–4 monolayers (ML) Pd/Fe(100) because of its higher symmetry and thereby its easier theoretical tractability. However, we regard the

underlying physics to be quite fundamental to the Pd-Fe interface rather than generated by a certain crystal geometry. By combining experimental and theoretical results we will show how the Pd electronic structure is influenced by the electronic and magnetic structure in the Fe substrate, and we will point out how this affects the photoemission spectra.

Our Fe(100) 3% Si picture frame single crystal has been prepared *in situ* by heating and Ne⁺ sputtering at 2 keV. In order to achieve optimum surface order the crystal was flashed to 370°C for 2 min. Although after this treatment no surface segregation of Si was detectable by Auger electron spectroscopy, 5 to 10 ML of Fe were evaporated onto the crystal prior to Pd overlayer preparation. Fe and Pd were evaporated by electron-beam heating at a rate of typically 0.17 ML/min. The sample was held at room temperature to prevent interdiffusion. Evaporation rates were measured with the use of a quartz crystal microbalance. The base pressure of the chamber was 1.8×10^{-10} mbar and raised during evaporation to 6×10^{-10} mbar. Monochromatic *s*-polarized synchrotron radiation from the TGM1 beamline at BESSY has been used to excite photoelectrons. Spin analysis has been performed with a 100-keV Mott detector. Majority and minority spin directions are defined with respect to the Fe valence-band population. Prior to each measurement the Fe(100) crystal has been remanently magnetized in the in-plane [010] easy axis, which was aligned to the spin-sensitive direction of the Mott detector. The photoemission spectra were taken at room temperature.

The growth of Pd on Fe(100) has been studied thoroughly by Auger electron spectroscopy and low-energy electron diffraction (LEED). The measured behavior of Pd and Fe Auger signals versus Pd deposition has been compared to model calculations, taking into consideration the possibility of island formation, surface segregation of Fe, and alloying at the Fe-Pd interface. Layer by layer (Frank-Van der Merwe) growth has been found for at least 5 ML. Surface segregation of Fe does not occur and no indication for interdiffusion at the interface was found. With LEED at 50.2-eV primary electron

energy the first-order diffraction spots were monitored: After deposition of 1-ML Pd the diffraction pattern does not differ from that of clean Fe neither with respect to arrangement nor to sharpness of the diffraction spots. At 2-ML coverage the pattern is still there although the spots have lost intensity. Still, no displacement of the spots occurs indicating that Pd adopts the 4.3% larger in-plane lattice constant of Fe. Eventually the LEED pattern and thus in-plane long-range order is lost during the growth of the third Pd layer.

Spin- and angle-resolved photoemission has been performed at 21-eV photon energy where the atomic photoionization cross section⁹ of the Pd 4*d* subshell is close to its maximum and about 5 times larger than that of Fe 3*d*. Figure 1 shows a selection of spin-resolved valence-band spectra at normal emission of clean Fe(100) and Pd coverages between 0.2 and 4 ML. The spectrum of the uncovered Fe reproduces earlier results,¹⁰ which were explained on the basis of a photoemission calculation.¹¹ From the 0.2-ML spectrum it can be seen how the effect of different cross sections for Fe 3*d* and Pd 4*d* enables us—in spite of the strongly overlapping valence-band emissions of Pd and Fe—to detect very low Pd coverages (● in Fig. 1). On increasing the Pd coverage, the Pd structure in the minority spin channel shifts, due to aug-

mented Pd-Pd coordination, from 2.6 eV at 0.2 ML towards lower binding energy with the peak (◇) dominating the *monolayer* minority spin spectrum located at 2.1-eV binding energy. Above 1-ML Pd coverage emission occurs more and more in the vicinity of the Fermi edge, and the *bulk* electronic structure has developed at 4 ± 0.5 ML.

Majority and minority spin channels of the monolayer spectrum in Fig. 1 are strongly different. This indicates that the monolayer Pd is magnetically polarized by the Fe substrate. Nevertheless, a pair of peaks spin split by the exchange interaction cannot be extracted directly from the monolayer spectrum. Instead, the minority spin channel is dominated by the comparatively sharp peak at 2.1 eV (◇) whereas the predominant structure of the majority spin spectrum is a broad peak with shoulders at 2.3, 1.75, and 0.8 eV.

At 1.3-, 1.6-, and 2.1-ML Pd coverage majority and minority spin spectra successively resemble each other, and eventually the 4-ML spectrum shows no net spin polarization anymore, indicating that the fourth Pd layer in the 4-ML system is not magnetically ordered anymore. In view of the kinetic energies involved in the photoemission process and the resulting probing depth of the photoelectrons, also the third Pd layer contributes to the 4-ML

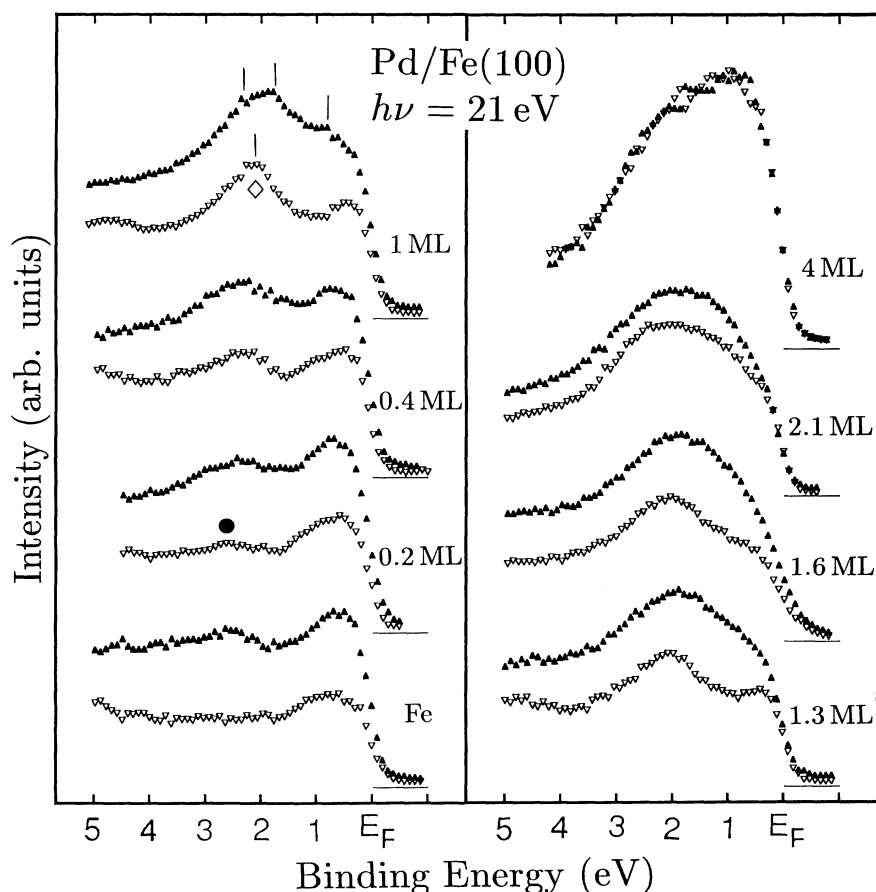


FIG. 1. Majority spin (▲) and minority spin (▽) valence-band spectra at 21-eV photon energy and normal emission with *s*-polarized light from clean Fe(100) and Pd coverages of 0.2 ± 0.05 , 0.4 ± 0.1 , 1 ± 0.1 , 1.3 ± 0.1 , 1.6 ± 0.1 , 2.1 ± 0.1 , and 4 ± 0.5 ML.

spectrum and is therefore expected to be nonmagnetic as well. For the same reason, the decrease of the spin polarization after the completion of the second Pd layer, which can be seen from the 2.1-ML spectrum, indicates that the surface Pd layer in the 2-ML system has a magnetic moment that is reduced with respect to the monolayer or even vanishes.

From now on we concentrate on the monolayer spectrum, and in order to provide an interpretation of its structures in terms of a band-structure model we have conducted an *ab initio* full-potential linearized augmented-plane-wave (FLAPW) calculation for a 9-layer Pd/7Fe(100)/Pd slab simulating 1-ML Pd on Fe(100). The magnetic moment of the Fe at the Pd-Fe interface was found to be $2.69\mu_B$, which is significantly larger than the calculated Fe bulk value of $2.15\mu_B$.¹² The Pd atoms gain a moment of $0.29\mu_B$.

On the other hand, a *paramagnetically* calculated Pd/7Fe(100)/Pd slab exhibits, for the Pd layer site, a density of states (not shown) at E_F that is much too small to give rise to a stable ferromagnetic Pd phase. Also, a Pd monolayer on Ag(100), for which the lattice expansion (5.1%) is even larger than for Pd/Fe(100) (4.3%), has been predicted to be paramagnetic.¹³ Therefore, perpendicular Pd-Fe hybridization, not lateral Pd-Pd hybridization, is considered responsible for the ferromagnetism within the Pd overlayer. This means physics is determined by the strong Pd-Fe interaction, and the Pd-Fe interface as a whole can be considered a new material with new properties.

Figure 2 shows the density of states (DOS), resulting from a ferromagnetic calculation, at the site of the Pd overlayer (solid line), and of the first underlying Fe layer (dotted line). The Pd 4*d* minority spin DOS of Fig. 2 is, similar to Ref. 14, not simply a replica of the majority

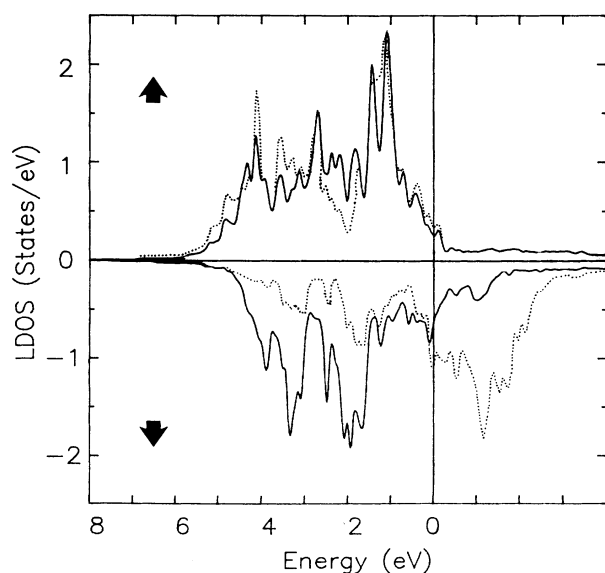


FIG. 2. FLAPW calculation for a Pd/7Fe(100)/Pd slab: Layer-resolved majority spin (\uparrow) and minority spin (\downarrow) density of states of the Pd overlayer on Fe(100) (solid line) and of the topmost Fe layer underneath the Pd (dotted line).

spin DOS shifted rigidly according to a Stoner model with constant exchange splitting. Obviously, Fe and Pd states are strongly overlapping in the majority spin direction, while for the minority spin direction the Fe DOS is shifted across E_F by about 2 eV due to exchange. Therefore, Pd 4*d*-Fe 3*d* hybridization at the interface is expected to be much stronger for majority spin electrons than for the minority spin electrons.

In our experimental geometry (*s*-polarized light, normal electron emission) we expect emission from states at the center of the two-dimensional Brillouin zone that are antisymmetric with respect to the surface normal, i.e., $\bar{\Gamma}_5$. In the calculation we take the cross-section argument into account when concentrating on those states whose wave functions lead to high probability in Pd muffin-tin spheres for electrons characterized by $\bar{\Gamma}_5$. In this way occupied states with more than 10% Pd 4*d* character are found at 2.68-, 1.83-, 1.41-, 0.95-, and 0.45-eV binding energy for majority and at 1.57 eV for minority spin. A complete matching of the energies between theory and experiment is obtained when shifting the calculated majority and minority spin bands rigidly by 0.5 eV to higher binding energies. This was done in Fig. 3 and is typical for the comparison of experimental band structures with those obtained by *ab initio* methods based on density functional theory. The pie charts of Fig. 3 contain, for the states in question, information on to which probability they are located at Pd sites. Obviously, only the $\bar{\Gamma}_5^{\downarrow}$ state identified with the peak at 2.1 eV is localized by 87% at the Pd layer

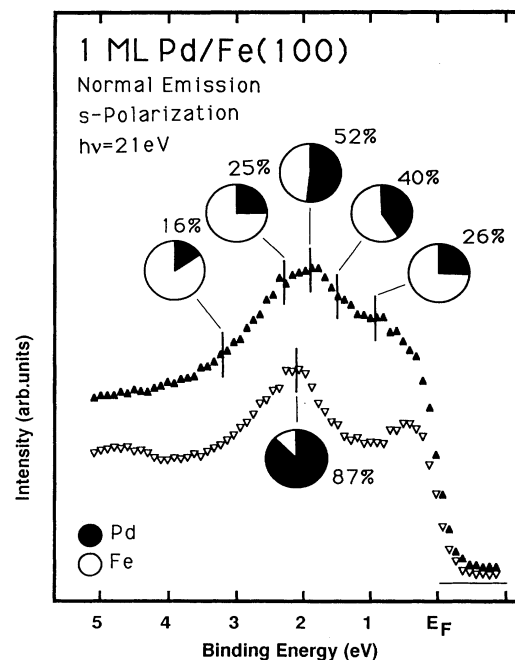


FIG. 3. Comparison between experiment and calculation: \blacktriangle and ∇ are experimental data of 1 ML Pd/Fe(100) taken from Fig. 1. Vertical bars represent the energy positions of $\bar{\Gamma}_5$ states obtained from the *ab initio* calculation after a shift of 0.5 eV towards higher binding energy. The pie charts indicate the calculated amount of Pd character in percent. (States with less than 10% Pd character are not shown.)

and therefore is of almost pure Pd $4d$ character. Recalling that the band structure of bcc material is split into bonding and antibonding states separated by a virtual gap we can identify the $\bar{\Gamma}_5^1$ states in Fig. 2 around the uppermost bonding state edge. But, in contrast to the deepest $\bar{\Gamma}_5^1$, the corresponding $\bar{\Gamma}_5^1$, exchange split by +1.1 eV, shows due to the strong $4d$ - $3d$ hybridization 84% Fe $3d$ character, which implies that for reasons of photoionization cross section this state is expected to be suppressed at 21-eV photon energy. On the other hand, the hybridization causes a distribution of the Pd character in the majority spin direction among the other $\bar{\Gamma}_5^1$ states at lower binding energies, where the predominant majority spin emission is observed in the spectrum.

In summary, we have found that up to 2 ML, Pd grows epitaxially on top of Fe(100). 1-ML Pd is ferromagnetically ordered on Fe. Our corresponding FLAPW calculation shows that the exchange-dependence of the Pd $4d$ -Fe $3d$ hybridization creates an electronic structure at the Pd-Fe interface that is twofold: The minority spin electronic structure of the Pd is only little affected by hybridization with the Fe. In contrast, in the majority electronic structure the hybridization leads to a spreading of the Pd $4d$ character among several states of identical symmetry. This is exactly reflected in the spin-resolved spectrum, where all of the predicted states appear, for reason of cross section, according to their quantity of Pd $4d$ character.

*Present address: BESSY GmbH, Lentzeallee 100, W-1000 Berlin 33, Germany.

¹S. Foner, R. Dolco, and E. J. McNiff, Jr., *J. Appl. Phys.* **39**, 551 (1968).

²T. Jarlborg and A. J. Freeman, *Phys. Rev. B* **23**, 3577 (1981).

³J. Crangle and W. R. Scott, *J. Appl. Phys.* **36**, 921 (1965); G. J. Nieuwenhuys, *Adv. Phys.* **24**, 515 (1975).

⁴B. Hillebrands, A. Boufelfel, C. M. Falco, P. Baumgart, G. Güntherodt, E. Zirngiebl, and J. D. Thompson, *J. Appl. Phys.* **63**, 3880 (1988); B. Hillebrands, P. Baumgart, and G. Güntherodt, *Appl. Phys. A* **49**, 589 (1989).

⁵V. L. Moruzzi and P. M. Marcus, *Phys. Rev. B* **39**, 471 (1989); L. Fritsche, J. Noffke, and H. Eckardt, *J. Phys. F* **17**, 943 (1987); H. Chen, N. E. Brener, and J. Callaway, *Phys. Rev. B* **40**, 1443 (1989).

⁶Ming Y. Zhu, D. M. Bylander, and Leonard Kleinman, *Phys. Rev. B* **42**, 2874 (1990).

⁷Z. Celinski, B. Heinrich, J. F. Cochran, W. B. Muir, A. S. Arrott, and J. Kirschner, *Phys. Rev. Lett.* **65**, 1156 (1990).

⁸W. Weber, D. A. Wesner, G. Güntherodt, and U. Linke, *Phys. Rev. Lett.* **66**, 942 (1991).

⁹J. J. Yeh and I. Lindau, *At. Data Nucl. Data Tables* **32**, 1 (1985).

¹⁰E. Kisker, K. Schröder, W. Gudat, and M. Campagna, *Phys. Rev. B* **31**, 329 (1985).

¹¹R. Feder, A. Rodriguez, U. Baier, and E. Kisker, *Solid State Commun.* **52**, 57 (1984).

¹²V. L. Moruzzi, J. F. Janak, and A. R. Williams, *Calculated Electronic Properties of Metals* (Pergamon, New York, 1978).

¹³S. Blügel, *Europhys. Lett.* **18**, 257 (1992).

¹⁴H. Huang, J. Hermanson, J. G. Gay, R. Richter, and J. R. Smith, *Surf. Sci.* **172**, 363 (1986).